Drop Breakup and Coalescence in Polymer Blends: The Effects of Concentration and Compatibilization†

Uttandaraman Sundararaj‡ and C. W. Macosko*

Department of Chemical Engineering and Materials Science, University of Minnesota, Twin Cities, Minneapolis, Minnesota 55455

Received August 18, 1994; Revised Manuscript Received December 19, 1994®

ABSTRACT: This study shows that a limiting dispersed phase particle size exists at very low concentrations for polymer blends mixed in an internal batch mixer and two types of twin-screw extruders. The Taylor limit for breakup of a single drop in a matrix underpredicts the limiting particle size; this discrepancy is attributed to viscoelastic effects. For uncompatibilized blends, the final particle size increases with the dispersed phase concentration due to increased coalescence. The particle size distribution also broadens at higher concentrations. Using *in-situ* reaction during blending or adding premade diblock copolymers suppresses coalescence resulting in smaller particle size and narrower particle size distribution. Using premade block copolymers is not as efficient in stabilizing morphology as using reactive polymers. It is shown that the main advantage of using compatibilizers in polymer blends is the suppression of coalescence achieved through stabilizing the interface, not a reduction in the interfacial tension. There is a critical shear rate in polymer systems where a minimum particle size is achieved. A qualitative explanation of why this occurs is given based on droplet elasticity.

Introduction

Polymer blends have provided an efficient way to fill new requirements for material properties.[1-3] The alternative to blending is synthesizing new polymers which not only involves exhorbitant costs but also cannot fulfill industrial demands.[3] Blending is done for a variety of reasons including creating materials with enhanced thermal and mechanical behavior. The great majority of useful blends are immiscible, and in these blends, mechanical properties can be optimized by controlling the blend morphology. Thus, the mixing that occurs in melt compounders like twin-screw extruders and batch mixers greatly affects the final product performance. Consequently, it is important to be able to predict how blending conditions will influence the blend morphology.

When two immiscible polymers are blended during melt extrusion, one phase is mechanically dispersed inside the other. The size and shape of the dispersed phase depends on several processing parameters including rheology, interfacial properties, and the composition of the blend. It has also been shown that blend morphology does not change significantly over time in batch mixers[4-8] and over length in twin-screw extruders after the initial period.[9] This invariant morphology is due to a rapid establishment of equilibrium between drop breakup and coalescence.[10-13] In polymer blends research, the drop breakup phenomenon has been studied extensively,[4-17] but coalescence has not been fully explored.[11,12,18-21]

In this paper, we investigate the importance of coalescence during melt blending. By changing the dispersed phase concentration, we can study the breakup–coalescence equilibrium during mixing. We can also probe the effect that compatibilizers such as diblock copolymers and reactive polymers have on the coalescence phenomenon. If the blend is mixed for sufficient time in a batch mixer, a stable morphology is reached. At low enough concentrations of the dispersed phase, only breakup should occur and there should be a limiting drop size. This limit can be calculated by balancing the shear and interfacial forces of an isolated drop in a matrix.

Background and Theory

Newtonian Drop Breakup. Taylor studied the breakup of a single Newtonian drop in a simple shear field.[22,23] He modeled drop size using viscosity ratio, $\eta_r = \eta_d/\eta_m$, and capillary number, Ca:

$$\mathrm{Ca} \equiv \dot{\gamma}\eta_m D/(2\Gamma) \tag{1}$$

where $\dot{\gamma}$ is the shear rate, η_m is the matrix phase viscosity, η_d is the dispersed phase viscosity, D is the diameter of the drop, and Γ is the interfacial tension.

For simple shear flow, Taylor balanced the interfacial forces and the shear forces and obtained a relation for the *maximum* drop size that would be stable:

$$D = \frac{4\Gamma(\eta_r + 1)}{\dot{\gamma}\eta_m\left(\frac{19}{4}\eta_r + 4\right)} \qquad \eta_r < 2.5 \tag{2}$$

This relation is valid for *small* deformations in Newtonian fluids. Many researchers have followed up Taylor's work.[14,24-32] Taylor predicted that no drop breakup occurs when $\eta_r > 2.5$. This result compares well with simple shear experiments[33-36] where no drop breakup was observed above $\eta_r = 4$.

For extensional flow, both experiments and theory[29-34] indicate that the critical capillary number, which can be thought of as an effective shear rate, is lower than that in the case of simple shear flow. The flow in mixers used for polymer blending is a mixture of simple shear flow and extensional flow. Thus, the critical capillary number for simple shear would predict the upper limit of drop size for breakup in a dilute Newtonian system.[32] Grace[34] has performed a monumental work on breakup of Newtonian drops in both simple shear and exten-

† Portions presented at AIChE Meeting, Los Angeles, Nov 1991, and Japan Society for Polymer Sciences, Morioka, Japan, Sept 1992. Presented at Polymer Processing Society Meeting, Akron, OH, March 1994.

‡ Present address: Department of Chemical Engineering, University of Alberta, Edmonton, Alberta T6G 2G6, Canada.

® Abstract published in *Advance ACS Abstracts,* February 1, 1995.

0024-9297/95/2228-2647$09.00/0

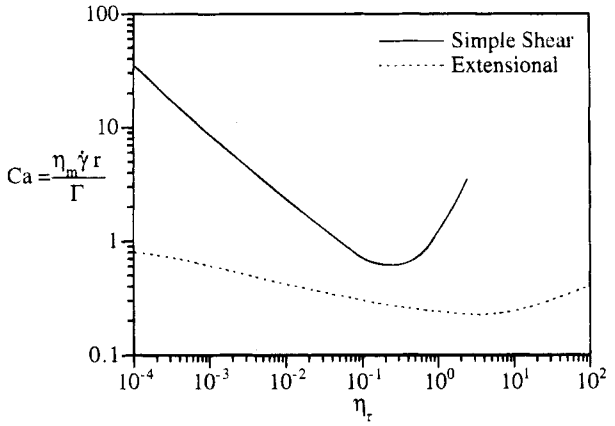

Figure 1. Newtonian drop breakup (adapted from Grace[34]). The experiments show that planar extensional flow is more effective at breaking drops than simple shear flow.

sional flows. These results are summarized in Figure 1. We see that breakup is possible in pure extensional flow at all viscosity ratios but is impossible in simple shear flow above $\eta_r = 4$.

Drop Breakup in Polymer Blends. The effect of viscosity ratio on drop size in melt blends has been investigated.[16,17,36] In these studies, the minimum dispersed phase concentration was 5 wt %; thus, the low concentration limit was not found. A correlation relating capillary number to viscosity ratio in extruded polymer blends has been given by Wu.[16] He gives a relation for the final particle diameter:

$$D = \frac{4\Gamma\eta_r^{\pm 0.84}}{\dot{\gamma}\eta_m} \tag{3}$$

where the plus (+) sign in the exponent applies for $\eta_r > 1$ and the minus (−) sign in the exponent applies for $\eta_r < 1$. In all blends used for the correlation, the dispersed phase concentration was 15 wt % and the effective shear rate was arbitrarily chosen as 100 s^{-1}. This relation obviously is not appropriate to the Taylor limit or to work on breakup of a single drop in a matrix (as in refs 14 and 22−35).

Newtonian Coalescence. Coalescence in binary Newtonian liquid mixtures has been examined by several researchers (including refs 37−50). It was found that the contact time required for drop coalescence increases when the drop diameter increases, the matrix viscosity increases, and the density difference between the drop and matrix phases increases.[47] Flow-induced coalescence of two Newtonian liquid drops can be modeled as a three-step mechanism[48] as shown in Figure 2. First, two drops come close to each other and the pair rotates in the shear field. The film of the matrix phase between the two drops drains, the film thickness decreases to a critical value, and rupture of the interface occurs, resulting in coalescence. Unlike gravity-induced coalescence, where the drops have time to equilibrate, contact times in shearing flows are small. Thus the film must drain very quickly for a droplet pair to coalesce.

Modeling of drop sizes during mixing has been done using population balance ideas similar to kinetic models.[51] Ramakrishna[52] has given an excellent review of population balance modeling of drop sizes in all engineering fields. In Newtonian systems, collision frequency (the number of times that particles meet) has been modeled satisfactorily, but coalescence probability

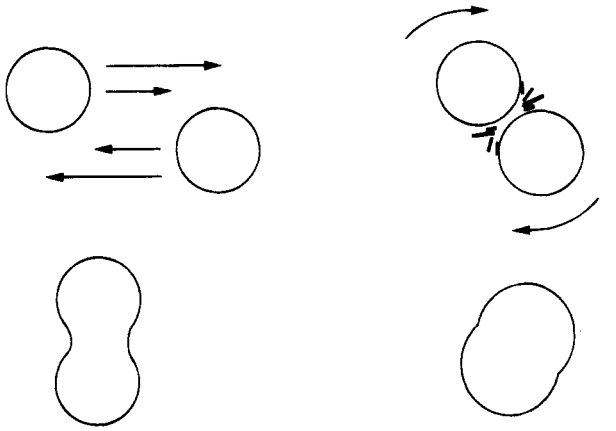

Figure 2. Idealized depiction of shear-induced coalescence of dispersed Newtonian droplets. The drops are brought close to each other by the shear field, and then the matrix film between the drops thins until the interface ruptures and coalescence occurs (adapted from refs 11 and 49).

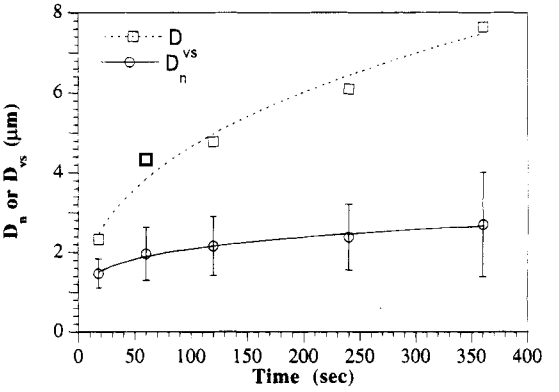

Figure 3. Quiescent coalescence in a polystyrene/polypropylene system (PS666D/PP3050 80:20). The annealing temperature was 180 °C. Zero shear rate viscosities: $\eta_{m,0} = 9500$ Pa·s, $\eta_{d,0} = 6000$ Pa·s. D_n is the number-average diameter, and D_{vs} is the volume-to-surface average diameter.

(the probability that the meetings result in coalescence) is still very empirical.[53] Coalescence probability in viscoelastic polymer systems is understood even less.

Coalescence in Polymer Blends. Most coalescence studies in polymer blends have not used mechanical mixing. Rather, they have studied coalescence in solvent-cast blends[19,54,55] or melt blends[7,19,20,56−62] under quiescent conditions. Coalescence after mixing is an important area since manufactured polymer products are often annealed and coalescence may occur during annealing. Coalescence in molten polymer blends without the influence of mechanical stress has been modeled by Fortelný and Kovář.[21] They found that the amount of coalescence in blends decreases significantly if the matrix phase viscosity is above a critical value and if the dispersed phase volume fraction is below a critical value. For typical particle sizes encountered in polymer blends (about 1 μm) and a 0.25 dispersed phase volume fraction, the model predicts that very little coalescence will occur above a critical maximum matrix viscosity of 496 Pa·s. However, we found significant coalescence within 10 min in an uncompatibilized polymer blend with a *lower* dispersed volume fraction of about 0.20 and a much *higher* matrix phase viscosity of 9500 Pa·s. The result is shown in Figure 3. The polymers were blended as described in the Experimental Section and then annealed at 180 °C. The sample preparation and particle size analysis are also described in the Experimental Section. The first data point is at 18 s since this

Table 1. Properties of Materials Used

polymer (abbrev)	source (functionality)	M_w	viscosity $\|\eta^*\|$ at 65 s^{-1} and 200 °C (kPa·s)
polystyrene (PS666D)	Dow Chemical	200 000	0.95, 0.22[a]
polypropylene (PP3050)	Elf Atochem	60 000 (M_n)	0.84
polypropylene (PP30875)	Elf Atochem		0.11
polyethylene (LDPE752)	Dow Chemical	194 000	0.400
ethylene–propylene (EP) 76% ethylene	Exxon	84 000	2.0
polystyrene–maleic anhydride (PSMA 17%)	ARCO (17% MA)	225 000	2.0, 0.33[a]
polystyrene–maleic anhydride (PSMA 1.5%)	Monsanto (1.5% MA)	185 000	0.85, 0.080[a]
amorphous polyamide (PA330)	Dupont (diamino functional)		10.0
polyamide-6,6 (PA6,6)	Dupont (diamino functional)		0.75[a]
polystyrene–oxazoline (PS–Ox)	Dow Chemical (1.0% oxazoline)	200 000	0.90
ethylene–propylene maleic anhydride (EP–MA)	Exxon (0.7% MA graft)	84 000	2.4
Kraton G 37% styrene (P(S–EP))	Shell	133 000	
Kraton G 32% styrene P(S–EP–S))	Shell	275 000	

[a] Viscosity at 270 °C.

was the time required to open the mixer. The volume-to-surface average particle size is shown to increase 3-fold within 6 min, and the particle size distribution broadens with annealing time. Other researchers have shown similarly dramatic coalescence effects in polymer blends.[7,19,20,54–62] The large coalescence effects seen during annealing of uncompatibilized blends indicate that polymers have a high interfacial mobility, i.e., that the interface is not rigid as one might expect for highly viscous fluids.

Coalescence during mixing will also be governed by the interfacial mobility. The interfacial mobility of polymers is described by van Gisbergen.[20] The high polymer matrix viscosity should give rise to a relatively immobile interface which should result in long drainage times for the intervening film. However, Elmendorp and van der Vegt[12] found experimentally that polymers had a high coalescence probability during mixing and concluded that polymers had fully mobile interfaces. Though a polymer matrix will have a high viscosity relative to a Newtonian matrix, drop collision and film drainage in polymer blends will be much different from the Newtonian model due to the different rheological behavior of polymeric liquids. Elastic recoil is expected to cause polymeric drops to separate during the initial collision step. However, Roland and Böhm[11] found that increasing shear rates, which intuitively one would expect to decrease coalescence, actually increased the amount of coalescence. Considering the properties of polymers, coalescence in polymer blends is much more significant than expected and it is clear that coalescence in polymer systems is not well understood.

Theoretical work[63–67] indicates that diblock copolymers located at the interface should be very efficient in compatibilizing blends by lowering the interfacial tension and stabilizing the morphology against coalescence. It has been reported that adding diblock copolymers to homopolymers lowers the interfacial tension between homopolymers from half to one-fifth the original value.[68–71] Another method of compatibilization is to use two polymers, each of which has a different chemical functionality along or at the end of the polymer chains. The two chemical functionalities can react with each other during the blending and form copolymer *in situ*. It has been reported that reactively formed copolymers also lower the interfacial tension.[71–73] However, the suppression of coalescence during annealing of compatibilized blends[57–61] suggests that copolymers (either premade or formed *in-situ*) prevent coalescence via steric stabilization. It has been shown that adding premade compatibilizers[6,58,74] or using a reaction at the interface[8,36,60,75,76] can significantly decrease the particle size at high dispersed phase concentrations. The studies did not separate between the effects of the compatibilization on coalescence and interfacial tension. Undoubtedly, the effect of compatibilizers on flow-induced coalescence has not been fully studied.

Experimental Section

Materials. All materials were provided in pellet form. The nominal shear rates in the mixer were found by assuming drag flow in the minimum and maximum gap between the mixer blades and the barrel. At a rotation rate of 50 rpm, the maximum shear rtate is calculated to be 65 s^{-1} and the minimum shear rate is 10 s^{-1}. The source, acronym, blend temperature, and magnitude of the complex viscosity, $|\eta^*|$, at 65 s^{-1} of the materials are given in Table 1. The dynamic rheological characterizations were performed using the Rheometrics RMS 800 rheometer with 25 mm parallel-plate fixtures at 10% strain. The polystyrene used in the experiments was Dow Styron 666D (PS666D). It is reported to have a melt index of 7.5 and has a molecular weight M_w = 200 000. Two polypropylenes were used: PP3050 and PP30875, both obtained from Elf Atochem. The low-density polyethylene used was Dow LDPE 752 (LDPE752), which has a M_w = 194 000. Ethylene–propylene rubber (EP) was Exxon EP V805 which has a M_w = 86 000 and 76% ethylene content.

Several nylons were used in the blends. One of the nylons used was Zytel 330 (PA330), which was provided by Dupont. It is a partially aromatic, amorphous nylon. Zytel 101 (PA6,6) is a nylon 6,6 obtained from Dupont. Several reactive polystyrenes were used: RPS XUS40056.01 (PS–Ox) with M_w = 200 000, provided by Dow Chemical Co., and two polystyrene–maleic anhydrides (PSMA) with differing maleic anhydride content. The PSMA with less maleic anhydride component is an experimental material obtained from Monsanto containing 1.5 wt % MA and having a M_w = 185 000.[77] The other PSMA is an Arco Dylark with 17 wt % MA having a M_w = 225 000. The reactive ethylene–propylene copolymer (EP–MA) obtained from Exxon is a maleic anhydride grafted material, and it has a M_w = 84 000. It is designated as XX1301. The diblock copolymer used in the P(S/EP) runs was Kraton G WRC 0021-89 from Shell. It is a P(S–EP) diblock with 37% styrene content and M_w = 133 000. The P(S–EP–S) symmetric triblock was Kraton G WRC 0023-89 which has 32% styrene content and M_w = 275 000.

Experiments. Before blending, all materials were heated at 80 °C under vacuum for 24 h to remove any volatiles. PA6,6 was heated at 140 °C. The Haake System 90 torque rheometer with a series 600 batch mixer and roller blades was used for all experiments. The mixer was preheated to the run temperature before adding the pellet mixture. The component weights were calculated by using the weight percents of each component and by requiring that the volume of material in the mixer at the operating temperature be kept at 54 cm^3. This corresponds to about 78% of the mixer's free volume. Using a glass frontal plate on the mixer to visualize mixing, we saw that at this loading there was optimal material interchange

Table 2. Experimental Runs, T = 200 °C

system (matrix/dispersed)	η_r viscosity ratio	Γ interfacial tension (10^3 N·m)	D Taylor limit (μm), Eq 2	D_n low conc limit (μm) (0.1% conc)
PA330/PS666D	0.10	18	0.03	0.25
PS666D/PA330	10.5[b]	18	0.25	0.67
PA6,6/PS666D[a]	0.29	7.5	0.15	0.92
PS666D/PP 3050	0.9	5.0	0.08	0.35
PP3050/PS666D	1.1	5.0	0.09	0.39
PP30875/PS666D	8.6[b]	5.0	0.60	1.81
PS666D/EP-MA	2.5	4.5	0.06	0.22
LDPE752/PS666D	2.3	4.9	0.17	0.50
		compatibilized runs		
PSMA17%/PA330	5[b]	18[c]	0.13	0.26
PA 330/PSMA1.5%	0.085	18[c]	0.03	0.10
PA6,6/PSMA17%[a]	0.44	7.5[c]	0.15	0.23
PA6,6/PSMA1.5%[a]	0.11	7.5[c]	0.15	0.25
PS−Ox/EP−MA	2.7	2.5	0.04	0.25
PS666D/P(S−EP)/EP diblock	2.1	2.3	0.03	0.20
PS666D/P(S−EP−S)/EP triblock	2.1	4.5[c]	0.06	0.25

[a] Run temperature = 270 °C. [b] Taylor[22] and others[25,33-36] predict no breakup at this viscosity ratio for Newtonian droplets in a simple shear field. [c] Interfacial tension for the uncompatibilized system.

between the mixer chambers and no stagnant areas at the center of the mixer.[78] The runs are summarized in Table 2. The concentration of the dispersed phase was varied from 0.1% to 8% for the PS/PP systems, from 0.1% to 30% for the PA6,6/PS systems, and from 0.1% to 15% for the PS/EP systems. Throughout this paper, blend systems will be reported as major (matrix) phase/minor (dispersed) phase.

After weighing out the required amounts of each component, the pellets were dry blended in a covered container. The mixer drive was set at 50 rpm. After 7 min of mixing, an equilibrium morphology was attained in the batch mixer for blend pairs at the conditions used.[8,9] After 12 min mixing, the motor was stopped and the front plate and the middle section of the mixer barrel were removed, exposing the mixer blades. The opening time varied from 15 to 25 s depending on the stiffness of the blend. A sample (~2 g) was taken from the indents in the mixer blades and was immediately quenched in liquid nitrogen. Using standard heat transfer equations for a 2-g sphere of polystyrene, it is found that the sample center temperature should cool from 200 °C to below 100 °C within 15 s after being dropped in liquid nitrogen.[8] We monitored the temperature using a thermocouple embedded in a 2-g homopolystyrene sample which was dropped into liquid nitrogen, and we found that the sample was quenched below 100 °C in less than 10 s.

The PS666D/PP3050 system has a viscosity ratio near unity. This should give the finest dispersion.[16] Experiments similar to those performed with the batch mixer were done with this system using a Haake TW100 conical counterrotating twin-screw extruder and a segmented Baker−Perkins corotating twin-screw extruder described previously.[9] The temperature, 200 °C, and rotation rate, 50 rpm, used in the conical extruder were the same as those used in the batch mixer. For the conical extruder, because of some of its narrow clearances, the average shear rates in the conical extruder and the batch mixer were matched. The maximum shear rates for the extruders were calculated assuming drag flow in the minimum gap between the screw (or kneading disk) and the barrel wall, and they were comparable to the maximum shear rate in the batch mixer. In the Baker−Perkins extruder, 25 rpm was used.[9] At this rotation rate, the maximum shear rate in the extruder was 65 s^{-1}, which matched the maximum shear rate in the batch mixer.

The PP30875/PS666D system (η_r = 8.6) was chosen to compare the breakup in polymer blends to that in Newtonian mixtures. Using eq 2, we see that no breakup occurs in Newtonian mixtures in simple shear flows when the viscosity ratio is greater than 4. The PA6,6/PS(-MA) systems provide results on the effect of reaction and the effect of increasing the number of functional groups on the chain. The PSMA17% has over 10 times as much functionality as the PSMA1.5%, but the added functionality could lead to cross-linking which may prevent drop breakup.

The PS/EP−MA system has no compatibilization and is compared to runs with PS−Ox/EP−MA, where a reaction can occur between the oxazoline and maleic anhydride groups,[79] and to runs using premade (S−EP) diblocks and triblocks. The diblock chain has an EP block that is about the same size as the EP homopolymer chain and a PS block which is about one-quarter the size of the PS homopolymer chain. The triblock chain has an EP block that is twice the length of the EP homopolymer chain and two PS blocks which are each one-quarter the size of the PS homopolymer chain.

When a premade block copolymer was used, the copolymer was first precompounded at 10 wt % concentration into the dispersed phase. The mixture was molded into plaques and cut into small cubes the size of pellets. The ratio of dispersed to matrix phase concentration was the same as in the uncompatibilized case. To achieve "x%" dispersed phase, the blend ratio was major/minor/copolymer, $(100 - y)$:0.9y:0.1y, where "y%" = "x%"/(0.9 + 0.001"x%"). The reactive blends were made in a one-step mixing as in the uncompatibilized case.

Sample Preparation and Analysis. To determine the average particle size, the samples were first extracted using a selective solvent[8] and then viewed under a scanning electron microscope (SEM). Either the matrix phase or the dispersed phase could be extracted. When the matrix was extracted, particles of the dispersed phase were suspended in solvent. A drop of this solution was placed on an SEM stub, and the solvent was allowed to evaporate. On the other hand, when the dispersed phase was to be extracted, a fracture surface of the blend was first obtained by freezing the sample in liquid nitrogen for 10 min and then breaking by bending. In many cases, a fracture surface would result when the hot blend sample from the mixer was immersed in liquid nitrogen. The fractured chunk was placed in solvent to extract the dispersed phase droplets, leaving holes in the matrix. The solvents used were methylene chloride to dissolve polystyrene and formic acid to dissolve nylon. All samples were sputter-coated with gold−palladium. Microscopy was done using the JEOL 840II HRSEM at 5 kV of accelerating voltage.

Extracting either phase allowed direct use of the Ultimage/X image analysis software (Graftek Inc., France) to find the number-average particle size. Each particle's diameter was determined from the areas found from the micrograph:

$$D_i = 2(A_i/\pi)^{1/2} \tag{4}$$

where A_i is the particle's area and D_i is its calculated diameter. Every point in Figures 3, 5, 7, 8, 10, and 12a is the average of 200−500 particles, except for the 0.1% concentration blends, where 75−100 particles were analyzed.

When the dispersed phase could not be selectively extracted, particle sizes were measured from micrographs obtained via two methods: using liquid nitrogen fracture surfaces like those

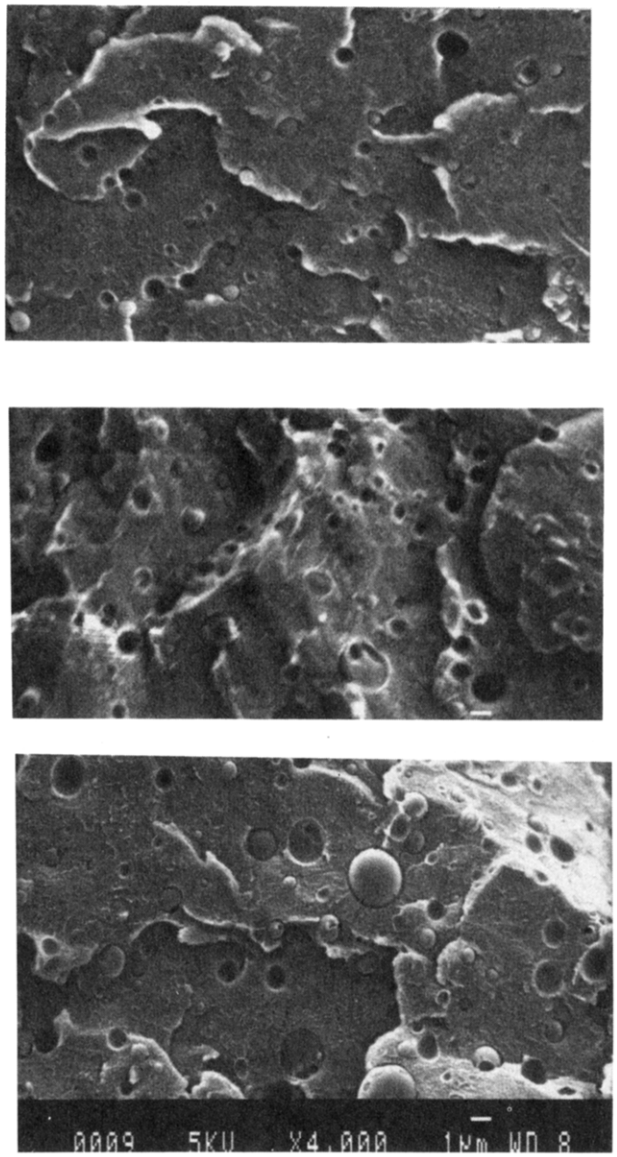

Figure 4. Micrographs of liquid nitrogen fracture surfaces of (top) 2, (middle) 5, and (bottom) 8 wt % PP3050 in PS666D mixed at 200 °C and 50 rpm for 12 min in the batch mixer. 1-μm marker is shown at the bottom.

shown in Figure 4 and/or isolating the dispersed particles by dissolving the matrix. For the fracture surfaces, a transparency was laid over the micrograph and the particles were traced by hand. The manual trace was then scanned into the image analysis software. There was very little difference (less than 10% in D_n) in the measured particle size using the fracture surfaces and the extracted samples, and the trends were not changed.

Corrections were done to the particle size found for microtomed samples using the Cruz-Orive method,[80] which is recommended by Russ.[81] Since there are several different particle sizes in a sample, a particle diameter seen on a microtomed section could be from a particle which has that diameter in all dimensions or, more likely, from a larger particle which has been sectioned away from its center. As well, for a certain section width, the number of small particles will be underrepresented since we will probably section through most of the larger particles and miss most of the very small ones. To find the diameters of the original spheres, a set of simultaneous equations relating the measured drop size distribution to the original sphere size distribution must be solved.[81]

For our particle size characterizations, the correction was done by first dividing the particle size distribution into 15 linear size ranges and characterizing each size range with the midpoint of the range. The measured particle size "vector" was then multiplied by a matrix of coefficients (obtained from ref 81) resulting from the solution of the set of equations to yield the sphere size distribution. Depending on the measured particle size distribution, the sphere size may be larger or smaller. Other corrections are available, but the solutions are similar.[81] The corrected values on the microtomed-thin-etched samples were compared with the uncorrected values for the same samples using the fracture surface or the isolated droplets. The difference in the average particle size was less than 10%, and the trends were unchanged; therefore, these corrections are neglected in the data presented.

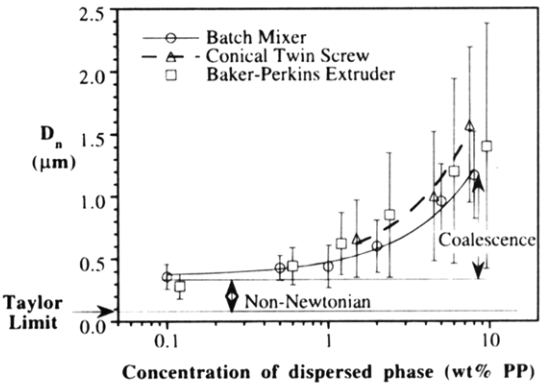

Figure 5. Number-average diameter of PP3050 particles in a PS666D matrix versus wt % PP3050. Results from both twin-screw extruders compare well to the batch mixer. The "error bars" are 1 standard deviation in each direction. The Taylor limit for the system is given in the plot. Viscosities are at 200 °C and 65 s^{-1}: η_m = 950 Pa·s, η_d = 840 Pa·s (from Table 1).

Results and Discussion

Batch Mixed Blends. Fracture surfaces of the PS666D/PP3050 system (η_r = 0.9) are shown in the micrographs in Figure 4. Figure 5 gives the particle size versus dispersed phase concentration for this system as well as the Taylor limit calculated from eq 2 (see also Table 2). The calculated drop size is 0.08 μm, consistent with literature experiments at the same viscosity ratio (η_r = 0.9).[34,82] In the low concentration limit, we attribute the discrepancy between Taylor's prediction of particle size and that observed in the experiment (D_n = 0.35 μm) to non-Newtonian effects. Polymers are highly elastic, and a drop of polymer tends to elongate significantly before breaking. The effect of drop phase elasticity on drop breakup is the same as that of increased interfacial tension.[14,83] Therefore, the limiting drop size for viscoelastic systems is larger than that predicted by eq 2. The "error bars" shown for each point in Figure 5 are 1 standard deviation in each direction for the particle sizes measured. Such bars are used in all figures to characterize the particle size distribution.

It should be noted that the maximum shear rate, $\dot{\gamma}$ = 65 s^{-1}, in the batch mixer was used to calculate the Taylor limit. This value was chosen since most of the breakup was expected to occur in the high shear rate region. The viscosity ratio of the PS666D/PP3050 system at 200 °C over the range of shear rates in the mixer is close to 1. Since the exact shear rate in the mixer is not known (it varies from 10 to 65 s^{-1}), we used all potential shear rates in eqs 2 and 3 to compare with the experimentally found average particle size. Figure 6 compares the Taylor limit and the prediction from Wu's correlation, at all potential shear rates, to the limiting diameter. The Taylor limit is lower than the experimental limit at all shear rates, while Wu's cor-

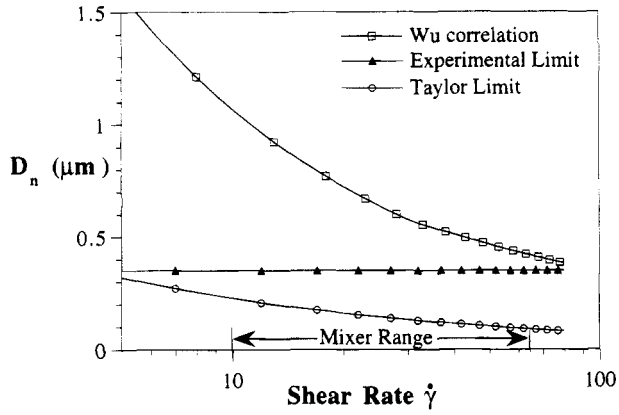

Figure 6. Theoretical limits at different possible shear rates in the mixer for the PS666D/PP3050 system. The low concentration limit found is always higher than the Taylor limit (eq 2) and is always lower than the result from Wu's correlation (eq 3).

relation is always higher. The Taylor limit has been found to be almost exact in drop breakup experiments using Newtonian liquid mixtures with viscosity ratios between 0.1 and 1.0 in simple shear flow.[34,82] The Taylor limit, however, does not account for the non-Newtonian effects that are present in this study. Polymer mixers have extensional flow in addition to simple shear flow, but extensional flows produce even finer dispersions than simple shear flows.[33,34] Therefore, the predicted limiting diameter would be even lower than the Taylor limit for simple shear flow.

In Figure 5, we see that, at higher concentrations of the dispersed phase, there are even larger discrepancies between the Taylor limiting particle size and the measured particle size. This difference results from coalescence that occurs in more concentrated blends. Coalescence can occur at low concentrations of the dispersed phase.[11] It can be seen in Figure 4 that, even though only 2 wt % polypropylene is present in the blend, some of the particles are very close to each other and droplet–droplet interactions occur during blending at these low concentrations. The blend pairs studied here suggest that, to neglect flow-induced coalescence, the dispersed phase concentration must be below 0.5%! For dispersed phase concentrations typically used in industrial blending (≥10%), the influence of coalescence on the final morphology will be even more pronounced than that seen in this study. It should be noted that local alterations of the flow field due to shielding near the particles may reduce the effectiveness of the flow field at higher concentrations. Figure 6 showed that the result from Wu's correlation is always greater than the experimental limit—this is due to coalescence at the high concentration (15%) which he used.[16] Though Wu's work gives a qualitative understanding of the effect of viscosity ratio on drop breakup behavior, it is not a fundamental result.

Another feature in Figure 5 is that the particle size distribution broadens at higher concentrations. This was true for all the uncompatibilized blends studied. Breakup and coalescence are occurring concurrently during the blending at the higher concentrations, resulting in a much broader distribution of drop sizes. Very small drops may result from breakup in the high shear regions, while increased coalescence due to more drop interactions will result in very large drops.

A similar study was done by switching the minor phase and major phase of the previous system so that

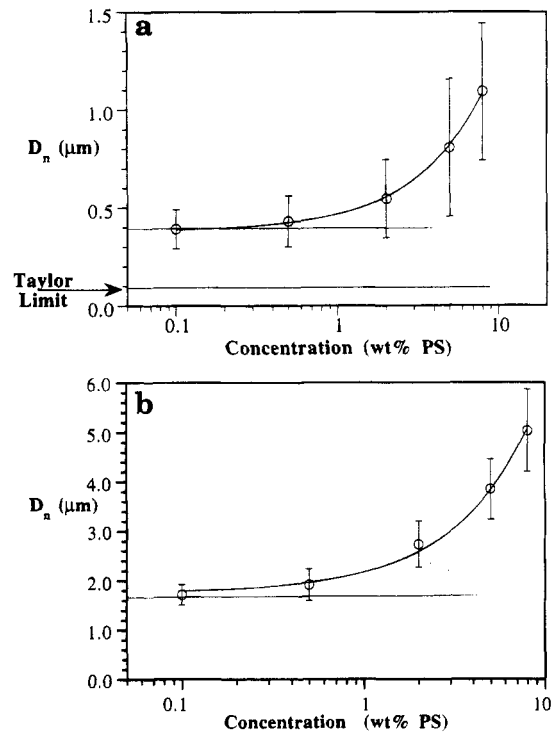

Figure 7. (a) Number-average diameter of PS666D particles in a PP3050 matrix versus wt % polystyrene (batch mixer, η_r = 1.1). The bars are 1 standard deviation in each direction. (b) Number-average diameter of PS666D particles in a PP30875 matrix (η_r = 8.6) versus wt % polystyrene.

η_r = 1.1. The coalescence plot is shown in Figure 7a. Since the viscosity ratio is hardly altered, we should obtain a similar particle size for the inverted system at the concentrations studied. The limiting particle size for the PP3050/PS666 system (D_n = 0.39 μm) shown in Figure 7a is identical within the bars to that shown for the PS666D/PP3050 system in Figure 5. The particle sizes at the higher concentrations are also comparable.

The results for another system using a lower viscosity polypropylene matrix, PP30875, with a PS666D minor phase (η_r = 8.6) are presented in Figure 7b. Again, coalescence increases the dispersed phase domain size as the concentration of dispersed phase increases. In addition, when a lower viscosity matrix is used to break up the same minor phase, larger domain sizes result. Equation 2 predicts that there will be no breakup for the high-viscosity ratio system; however, breakup does occur in the experiment, and the low concentration limit is about 1.8 μm. Extensional flows in the batch mixer may have been responsible for drop breakup at η_r > 4.[23,33,34,82] However, the unique manner in which viscoelastic materials deform may also have been important.[8,9,84]

Blending in a Twin-Screw Extruder. Twin-screw extruders are used in industry for polymer blending. To compare the dispersions obtained with the batch mixer, we mixed the same PS666D/PP3050 system in two different extruders, and the results are plotted in Figure 5. The limiting particle size is the same as that found for the batch-mixed case. With the same maximum shear rate, the particle sizes in blends with low dispersed phase concentrations prepared with the two types of mixers are comparable. Figure 5 also shows that, with increasing concentration, the particle size increases, just as in the batch-mixed blends. At higher concentrations, increasing the dispersed phase concentration in the extruder results in a greater increase in

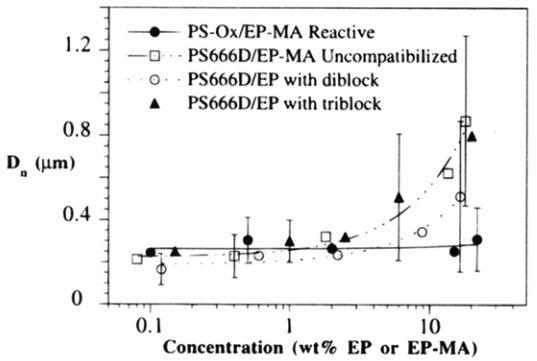

Figure 8. Effect of compatibilization on coalescence for the polystyrene/ethylene–propylene system. The uncompatibilized blend behaves similarly to the other blend systems (Figures 5 and 7). All PS/EP blends have similar diameters at low concentrations, but adding premade diblock or using reactive components suppresses coalescence at the higher concentrations. Reaction is extremely effective at eliminating coalescence.

the particle size and a greater increase in the breadth of the particle size distribution than that found in the batch mixer experiments. This is attributed to the "flow-through" nature of extruders. Thus, we need to study not only the coalescence phenomenon but also the escape of large droplets from the mixer which would have broken up under the imposed shear at longer residence times. Because of the escape of these large particles, the particle size distribution is much broader. Therefore, the effects of coalescence and drop escape are difficult to separate when using the twin-screw extruder. The extruder could be used to study coalescence by running the material through the extruder several times until a steady-state morphology is achieved. This procedure requires much more work than using the batch mixer and will at best provide similar results.[12]

Effect of Block Copolymers. The effect of block copolymers on blend morphology was studied using a commercial diblock P(S–EP) copolymer and a commercial triblock P(S–EP–S) copolymer which we felt would compatibilize PS666D/EP blends. The results are shown in Figure 8. The limiting particle size is the same as that of the uncompatibilized case for these blends, and the particle size still increases with concentration. The diblock copolymer suppresses coalescence somewhat at higher concentrations but does not affect the particle size distribution greatly. The triblock has no effect on either the particle size or the particle size distribution and follows the uncompatibilized curve almost exactly. Both types of block copolymers are shown to be poor compatibilizing agents for the PS666D/EP blend.

If the block copolymer lowers the interfacial tension, then at low concentrations, the particle size of the compatibilized blend should be significantly smaller than that of the uncompatibilized blend, since lowering the interfacial tension will decrease the interfacial stress whereas it does not affect the matrix shear stress (see eqs 2 and 3). Since the limiting particle sizes for the blends with copolymer are identical to the limiting particle size in the uncompatibilized blend, the main, or rather the only, advantage gained by using the copolymer is steric stabilization against coalescence at higher concentrations.

When we add a A–B diblock copolymer to a A/B homopolymer blend, we assume that the diblocks will diffuse to the interface during the blending. This may occur in low molecular weight polymers and in Newtonian emulsions. However, when the chains are long, $N > 1000$, diffusion times are much longer and, within the mixing time, the diblock may stay in a micelle inside one phase rather than migrate to the interface. Thermodynamically, the diblock should prefer the interface,[63–67] but the shear forces may not be sufficient to break up the large micelles. In our blends, the block copolymer was preblended with the EP, and the PS block components most probably formed micelles. However, it should be noted that the microstructure of the hydrogenated isoprene in the diblock copolymer has a much lower ethylene content than the EP rubber. Therefore, the EP rubber and the EP block of the copolymer will not be miscible. During the blending, some copolymer may have reached the interface as indicated by the slight suppression of coalescence seen in Figure 8. It should be noted that changing the lengths of each component or changing the overall diblock length may give different behavior.

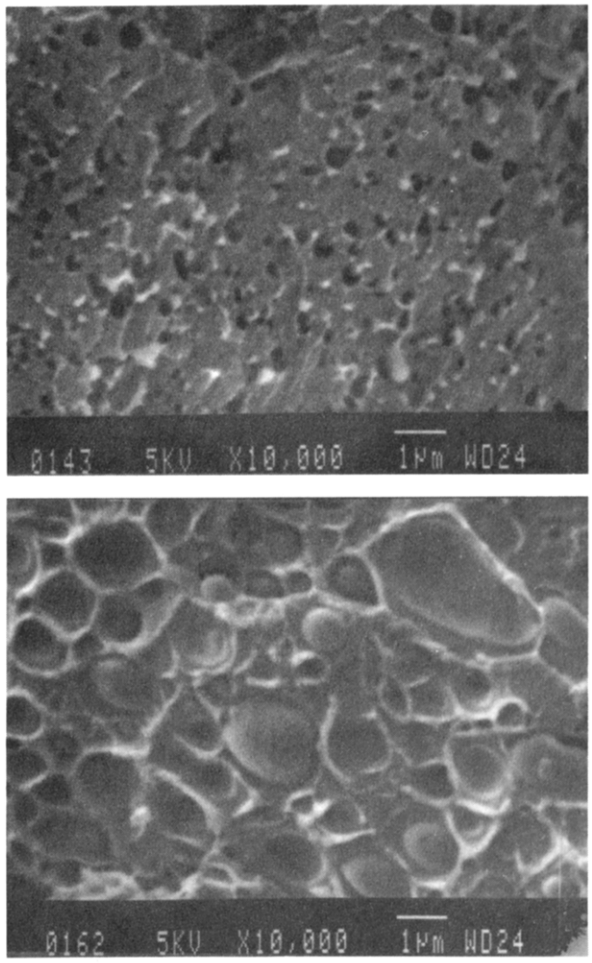

Figure 9. Effect of reaction on morphology in PS/EP system (85:15): (bottom) uncompatibilized PS666D/EP-MA exhibits coarse morphology, (top) reactive PS-Ox/EP-MA shows a much finer morphology. 1 μm marker shown.

Effect of Reaction. The morphologies of the reactive and uncompatibilized PS/EP systems at a dispersed phase concentration of 15 wt % are compared in Figure 9. The particle size is much smaller in the reactive case. Also, the fracture itself is rougher when there is a reaction. The particle size versus concentration for the reactive PS–Ox/EP–MA system is shown in Figure 8. The particle size in the low concentration limit is again the same as that in the uncompatibilized case. However, the particle size does not change throughout the

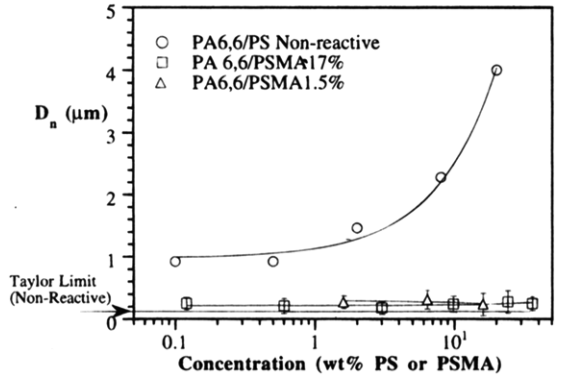

Figure 10. PA6,6/PS(-MA) systems. Number-average diameter versus wt % dispersed phase. Using 1.5% or 17% reaction gives very similar results. *In-situ* reaction decreases the low concentration limit and eliminates coalescence at the higher dispersed phase concentrations. The Taylor limit for the nonreactive system is given. Viscosities are at 270 °C and 65 s^{-1}: $\eta_{PS666D} = 220$ Pa·s, $\eta_{PSMA1.5\%} = 80$ Pa·s, $\eta_{PSMA17\%} = 330$ Pa·s, $\eta_{PA6,6} = 750$ Pa·s. No bars are shown for the PA6,6/PS system because the particle size distribution is too broad to fit in the figure.

entire range of concentrations used. Therefore, when reactive polymers are used, coalescence is eliminated at high concentrations so that the particle size at 20 wt % concentration is identical to the 0.1 wt % particle size. This is an important result, since it shows that the most significant effect of the *in situ* formed copolymers is to reduce coalescence at higher concentrations.

Breakup of a single droplet in a matrix can be used to calculate the relative interfacial tensions if the viscosities and shear rate are known.[35] From Figure 8, we see that the particle sizes at the low concentration limit for reactive and uncompatibilized systems are almost identical within the bars (that is, within 1 standard deviation of the respective distributions). If interfacial tension was significantly lowered, then the limiting drop size would have decreased. When we attempted to measure the interfacial tension through the breaking thread method[69,71] for the reactive and added diblock systems, we found a reduction in interfacial tension to about half the value obtained for the uncompatibilized system (see Table 2). The result is comparable to other studies.[68-73] This decrease in interfacial tension is not enough to account for the 5-fold decrease in particle size at 20 wt % concentration seen in Figure 8 or the 20-fold decrease shown in Figure 10.

Figure 10 again demonstrates the power of using interfacial reaction to stabilize morphology during processing. The particle size at 20 wt % for nonreactive PA6,6/PS666D is 4 times the limiting particle size at low concentration for the uncompatibilized system. The experimental limit at low concentration is 5 times as large as that predicted from Taylor's theory; we propose that this is due to viscoelastic effects. The striking result in Figure 10 is that the reactive blend dispersions of the PA6,6/PSMA systems are stable during processing throughout the concentration range studied, and this is the case for both 1.5 wt % MA functionality and 17 wt % MA functionality. Thus, very little reaction is required to produce a significant effect on the morphology. Angola *et al.*[76] showed that, at 1.5 wt % functionality, a minimum particle size was achieved for nylon 6/PSMA blends. Other work has shown effective morphology stabilization[60] even for end-functional materials—where there is only one functionality per chain. The reactive groups go to the interface and form

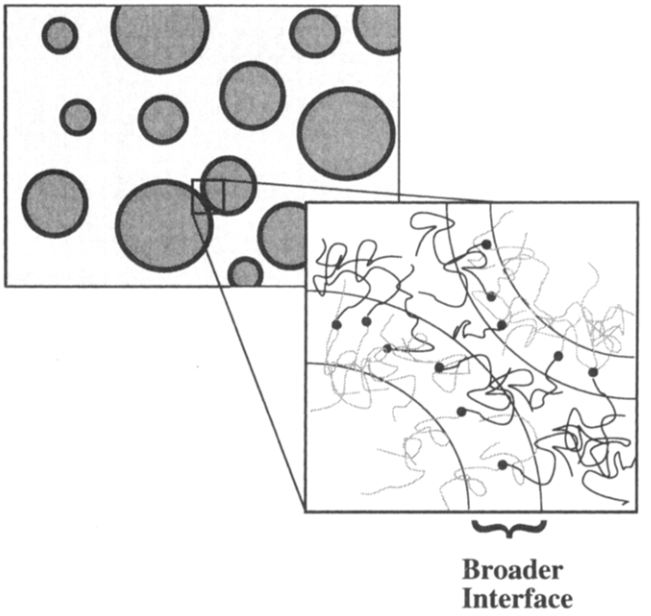

Figure 11. Suppression of coalescence. Two drops which have a layer of diblock or graft copolymer at the interface are less likely to coalesce since copolymer molecules form shells around the drops.

sufficient copolymer so that, even at high dispersed phase concentrations, the dispersed phase domains act like isolated droplets in an infinite medium.

It has been shown that when surfactants are used in Newtonian emulsions, there is an increase in the energy required for coalescence partly due to steric interactions of adsorbed layers at the liquid–liquid interface.[45,85,86] The stabilization against coalescence for compatibilized polymer blends is similar in nature and is shown schematically in Figure 11. The interface consists of a layer (or layers) of copolymers. Based on thermodynamic arguments,[86] the block segment of the matrix phase polymer is located on the outside of the drop since it is incompatible with the drop. Therefore, one can imagine the dispersed phase drop with a shell of copolymer, with the outside consisting of matrix phase block segments. When the matrix fluid tries to drain as the drops come together, the copolymers at the interface do not allow the dispersed phase in the two drops to meet and the drops recoil. In order for the dispersed phase in the two drops to meet, the copolymers must be moved out of the contact area. Since the interfacial viscosity increases upon adding a compatibilizer,[85] it will be difficult to move the copolymers—thus, coalescence is retarded. If there is enough copolymer at the interface, then it may form an "interphase" which must be overcome for coalescence to occur. However, the interface does not necessarily need to be saturated with diblock or graft copolymer to be effective—we only require that amount of copolymer which will provide enough steric interactions to prevent droplets from coalescing.

A striking feature in Figure 10 is that the limiting particle size for the reactive blends is significantly smaller than that of the uncompatibilized blend—the particles in the reactive blend are about one-quarter the size of the nonreactive counterpart. This may be due to a reduction in the interfacial tension. We could not measure the interfacial tension in the reactive blends with the breaking thread method since the interface cross-linked and the thread remained stable for several hours. However, during the initial stage of blending

where the materials soften and melt, the amine–maleic anhydride reaction in the PA6,6/PSMA system is very fast.[77] This reaction generates copolymers which may influence the blend morphology. Thus, the reactive blend can exhibit a finer dispersion than the nonreactive blend in the low concentration limit due to the reaction. The copolymers formed from this reaction then stabilize the fine dispersion regardless of the dispersed phase concentration.

It is interesting that Figure 8 does not show the same discrepancy between the limiting particle size for the reactive and nonreactive systems as seen in Figure 10. It has been shown that the oxazoline–maleic anhydride reaction is not as fast as the amine–maleic anhydride reaction.[8,88] The oxazoline–maleic anhydride reaction occurs in the PS–Ox/EPMA after the initial softening region, where most of the morphological change occurs.[4–9] Thus, the reaction in the PS–Ox/EPMA system does not affect the initial morphology generation; rather, it stabilizes the finest dispersion possible which is the low concentration limit of the uncompatibilized blend.

Table 2 summarizes the diameters found for the low concentration limit for both compatibilized and uncompatibilized materials. Table 2 includes the results for another system, PS/PA330. This system also showed that reaction eliminated the coalescence at higher concentrations of the dispersed phase. Note that when the interfacial tension could not be measured for compatibilized systems, the tabulated Taylor limit was calculated using the value for the uncompatibilized blend. This, of course, will lead to predicted diameters much larger than those if the reduced interfacial tension is used.

Effect of Shear Rate. Equation 2 indicates that we can decrease the size of the drops by continually increasing the shear rate. We performed such an experiment with the PS666D/PP3050 system (92:8 concentration ratio), and the results are shown in Figure 12a. The PS666D/PP3050 system was chosen because, over a wide range of shear rates, the viscosity ratio was approximately unity. Therefore, the effects of the viscosity ratio can be neglected in the results presented in this section. For the 8% dispersed phase, a minimum particle size is reached when the (maximum) shear rate in the mixer is 130 s^{-1}, and at higher shear rates, the particle size actually increases. This anomaly has been reported by other researchers,[6] or has been shown and the authors have made no comments.[17,87] Polymer melts are shear-thinning materials, so that when the shear rate is increased, the matrix viscosity can decrease sharply. The simple power law constitutive equation applied to steady simple shear flows describes the shear-thinning behavior quite well at the high shear rates typically found in polymer mixers:

$$\tau_m = \eta_m \dot{\gamma} = M\dot{\gamma}^n \tag{5}$$

τ_m is the matrix shear stress, M is the power law coefficient, and n is the power law index ($0 < n < 1$). The viscosity never thins as fast as the shear rate is increased, and thus from eq 5, we see that the matrix shear stress continues to increase as shear rate increases. Though the shear-thinning characteristic of polymers explains why the size does not monotonically decrease, it cannot describe why particle size should *increase*.

The unexpected behavior may occur in this system for two reasons: coalescence and viscoelasticity. We have already demonstrated that coalescence occurs in

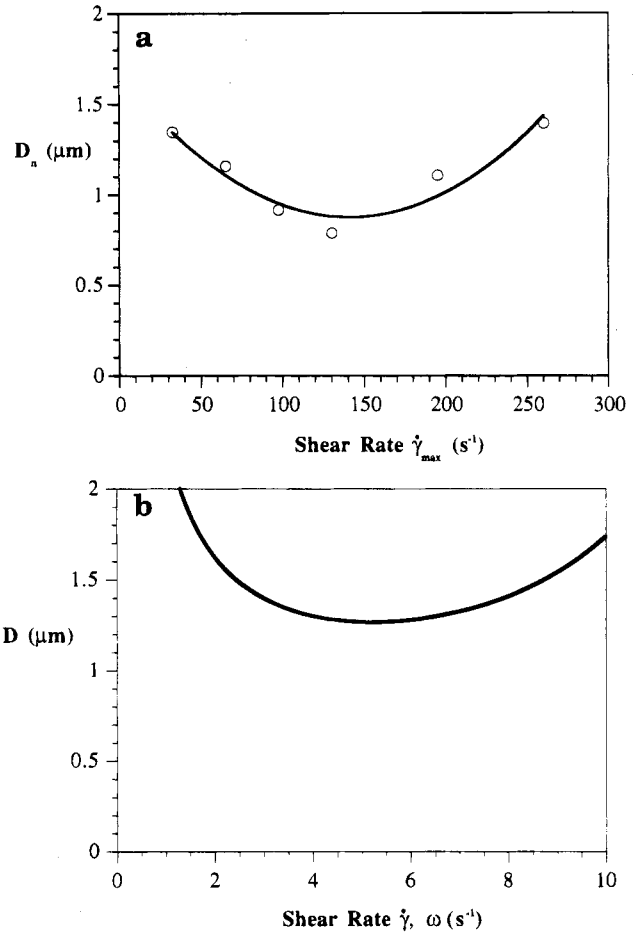

Figure 12. (a) Diameter versus shear rate in PS666D/PP3050 (92:8). Blending temperature was 200 °C. The effect of shear-induced coalescence is seen at the higher shear rates. (b) Prediction of drop size using the balance between drop deforming and drop restoring forces (eq 7). Elastic effects may be responsible for this behavior.

polymer systems at concentrations higher than 0.5%. At 8% dispersed phase concentration, there is significant coarsening. For example, in Figure 5, at 8 wt % concentration, the particle size is about 3 times the low concentration limit. At higher shear rates, the droplets have higher approach velocities and thus the coalescence probability can increase.[11]

The reason why we see a minimum can also be explained by a critical drop size which may exist in viscoelastic systems.[82] If we consider that the matrix viscous forces deform the drop whereas the interfacial forces and the drop elasticity resist this deformation, we can predict when breakup will occur:

$$\eta_m \dot{\gamma} > \mathrm{Ca}_{crit}(2\Gamma/D) + N_1 \tag{6}$$

where Ca_{crit} is the capillary number at breakup and N_1 is the first normal stress difference. By rearranging the balance, we can find the drop size that can be achieved:

$$D > \frac{2\Gamma \mathrm{Ca}_{crit}}{\eta_m \dot{\gamma} - N_1} \tag{7a}$$

Now $\mathrm{Ca}_{crit} \sim 0.5$ at $0.1 < \eta_r < 1.0$ and the elastic forces can be approximated by $N_1 = 2G'_d$, the dynamic modulus, at low shear rates and low frequency. The diameter can be found at every shear rate using eq 7a, and it is plotted in Figure 12b. At the shear rate where the elastic restoring forces are less important compared

to the matrix shear force deforming the drop (i.e., the difference $\eta_m\dot{\gamma} - 2G'_d$ in eq 7a is maximum), we see that there is a minimum drop size:

$$D_{min} = \frac{\Gamma}{\eta_m\dot{\gamma}_{cr,min} - 2G'_d(\omega=\dot{\gamma}_{cr,min})} \quad (7b)$$

where ω is the frequency at which G'_d is measured and $\dot{\gamma}_{cr,min}$ is the critical shear rate where this minimum occurs.

For the PS666D/PP3050 system, the denominator in eq 7a is maximized when the shear rate is 6 s^{-1}. At this critical shear rate we find the minimum drop size, which is calculated from eq 7b to be 1.25 μm. Below this drop size, no drop breakup by the classical mechanisms[22-35] should occur. The increase in particle size at higher shear rates is also explained through this analysis. However, the similarity of parts a and b of Figure 12 is only qualitative. A notable deficiency in eq 7b is that the simple relation for the elastic forces, $N_1 = 2G'$, cannot be used at higher shear rates. Nonetheless, the result shows that, in polymer systems, the behavior is significantly different from the classical Newtonian systems and more modeling work is required in the area to properly describe breakup and coalescence phenomena. The data presented in this work provide an experimental basis for further modeling efforts.

Conclusions

This study shows that a limiting dispersed phase particle size exists in polymer blends for surprisingly low dispersed phase concentrations ($\leq$0.5%). The final particle size depends on the dispersed phase concentration, especially for uncompatibilized blends. Coalescence during the blending process occurs at higher concentrations, resulting in larger particle sizes. In all the blends studied, there were broad distributions in particle size. Breakup occurred in the PP30875/PS666D system ($\eta_r = 8.6$) and the PS666D/PA330 system ($\eta_r = 10.5$), though Taylor and others predict[22,25] and observe[23,33-35,82] that (Newtonian) drops do not break up in simple shear flows at viscosity ratios above $\eta_r = 4$. The Taylor limit (eq 2) does not accurately predict the particle size for polymer blends mixed in the batch mixer at low dispersed phase concentrations. The discrepancy is attributed to polymer viscoelastic effects. Equation 7 tries to include the elastic portion in the drop breakup force balance. There is a critical minimum drop size as shear rate is varied, and this can be accounted for through the polymer elasticity (eq 7). When shear rate is increased, the matrix viscosity decreases and the drop elasticity increases, so that the drop resists the deformation to a greater extent. Consequently, there is an optimum shear rate where the finest dispersion is obtained. We have shown that polymer systems behave very differently from Newtonian systems.

The blend morphology at the exit of the twin-screw extruder includes large drops which have "escaped" the high shear regions. The differences in particle size between the different concentrations are due to the effects of coalescence and the drop escape frequencies in the twin-screw extruder. Thus, the particle size is slightly larger and the particle size distribution is much broader for the twin-screw extruder than for the batch mixer. These results agree with models for Newtonian mixtures in batch and continuous mixers.[37]

Adding diblock copolymers or using reactive blends suppresses coalescence at higher concentrations. Reaction is more efficient since it eliminates coalescence effects at concentrations up to 30 wt %—the highest concentration studied. It is shown that very little reaction (even 1 wt % reactive component) is sufficient to stabilize the morphology during blending. The diblock copolymer, though it does reduce coalescence, gives very broad particle size distributions and larger average particle sizes compared to the reactive blend. This work shows that the main contribution from added premade diblock copolymers or interfacial reaction in blends is a suppression of coalescence not a reduction of interfacial tension. There may be a reduction in interfacial tension, but in industrial blends which usually have higher concentrations of dispersed phase (10–50%), this reduction is not nearly as important as the elimination of coalescence through interfacial stabilization.

Acknowledgment. The authors thank Mr. Paul Gilbert for preparing some of the blends and Ms. Carmen Stern for performing image analysis. The authors thank Prof. F. S. Bates and Prof. M. Tirrell for helpful discussions regarding the role of block copolymers in compatibilization. U.S. is grateful to Plastics Institute of America for supplemental research fellowships. This work was carried out under grants from the 3M Company and General Electric as well as the NSF Grant CTS-9203108 (Chemical Reaction Processes and the Polymer Program of the Materials Division).

References and Notes

(1) Utracki, L. A. *Polym. Eng. Sci.* **1983**, *23*, 602. Utracki, L. A. *Polymer Alloys and Blends*; Hanser Publishers: Munich, 1989.
(2) Rätzch, M. *Makromol. Chem., Macromol. Symp.* **1987**, *12*, 165.
(3) Meijer, H. E. H.; Lemstra, P. J.; Elemans, P. H. M. *Makromol. Chem., Macromol. Symp.* **1988**, *16*, 113.
(4) Karger-Koscis, J.; Kalló, A.; Kuleznev, V. N. *Polymer* **1978**, *19*, 448.
(5) Schreiber, H. P.; Olguin A. *Polym. Eng. Sci.* **1983**, *23*, 129.
(6) Plochocki, A. P.; Dagli, S. S.; Andrews, R. D. *Polym. Eng. Sci.* **1990**, *30*, 741.
(7) Favis, B. D. *J. Appl. Polym. Sci.* **1990**, *39*, 285.
(8) Scott, C. E.; Macosko, C. W. *Polym. Bull.* **1991**, *26*, 341; *Polymer* **1995**, *36*, 000. Scott, C. E. Ph.D. Thesis, University of Minnesota, Minneapolis, MN, 1990.
(9) Sundararaj, U.; Macosko, C. W.; Rolando, R. J.; Chan, H. T. *Polym. Eng. Sci.* **1992**, *32*, 1814.
(10) Nelson, C. J.; Avgeropoulos, F.; Weissert, F. C.; Böhm, G. G. A. *Angew. Makromol. Chem.* **1977**, *60*, 49.
(11) Roland, C. M.; Böhm, G. G. A. *J. Polym. Sci., Polym. Phys.* **1984**, *22*, 79.
(12) Elmendorp, J. J.; van der Vegt, A. K. *Polym. Eng. Sci.* **1986**, *26*, 1332.
(13) Lyngaae-Jørgensen, J.; Valenza, A. *Makromol. Chem., Macromol. Symp.* **1990**, *38*, 43.
(14) Chin, H. B.; Han, C. D. *J. Rheol.* **1980**, *24*, 1.
(15) Min, K.; White, J. L.; Fellers, J. F. *J. Appl. Polym. Sci.* **1984**, *29*, 2117.
(16) Wu, S. *Polym. Eng. Sci.* **1987**, *27*, 335.
(17) Favis, B. D.; Chalifoux, J. P. *Polym. Eng. Sci.* **1987**, *27*, 1591.
(18) Tokita, N. *Rubber Chem. Technol.* **1977**, *50*, 292.
(19) Jang, B. Z.; Uhlmann, D. R.; van der Sande, J. B. *Rubber Chem. Technol.* **1984**, *57*, 291.
(20) van Gisbergen, J. Ph.D. Thesis, Eindhoven University of Technology, Eindhoven, The Netherlands, 1991.
(21) Fortenlý, I.; Kovář, J. *Polym. Compos.* **1988**, *9*, 119.
(22) Taylor, G. I. *Proc. R. Soc. London* **1932**, *A138*, 41.
(23) Taylor, G. I. *Proc. R. Soc. London* **1934**, *A146*, 501.
(24) Cox, R. G. *J. Fluid Mech.* **1969**, *37*, 601.
(25) Barthès-Biesel, D.; Acrivos, A. *J. Fluid Mech.* **1973**, *61*, 1.
(26) Bentley, B. J.; Leal, L. G. *J. Fluid Mech.* **1986**, *167*, 219.
(27) Flumerfelt, R. W. *J. Colloid Interface Sci.* **1980**, *76*, 330.
(28) Hinch, E. J.; Acrivos, A. *J. Fluid Mech.* **1980**, *98*, 305.
(29) Rallison, J. M. *J. Fluid Mech.* **1981**, *109*, 445.
(30) Acrivos, A.; Lo, T. S. *J. Fluid Mech.* **1978**, *86*, 641.

(31) Chin, H. B.; Han, C. D. *J. Rheol.* **1979**, *23*, 557.
(32) Bentley, B. J.; Leal, L. G. *J. Fluid Mech.* **1986**, *167*, 241.
(33) Karam, H. J.; Bellinger, J. C. *Ind. Eng. Chem. Fundam.* **1986**, *7*, 576.
(34) Grace, H. P. *Chem. Eng. Commun.* **1982**, *14*, 225.
(35) Rumscheidt, F. D.; Mason, S. G. *J. Colloid Sci.* **1961**, *16*, 238.
(36) Serpe, G.; Jarrin, J.; Dawans, F. *Polym. Eng. Sci.* **1990**, *30*, 553.
(37) Coulaloglou, C. A.; Tavlarides, L. L. *Chem. Eng. Sci.* **1977**, *32*, 1289.
(38) Jeelani, S. A. K.; Heartland, S. *Chem. Eng. Sci.* **1991**, *46*, 1807.
(39) Park, J. Y.; Blair, L. M. *Chem. Eng. Sci.* **1975**, *30*, 1057.
(40) Park, J. Y.; Crosby, E. J. *Chem. Eng. Sci.* **1965**, *20*, 39.
(41) Charles, G. E.; Mason, S. G. *J. Colloid Sci.* **1960**, *15*, 236.
(42) MacKay, G. D. M.; Mason, S. G. *J. Colloid Sci.* **1963**, *41*, 203.
(43) Burrill, K. A.; Woods, D. R. *J. Colloid Interface Sci.* **1973**, *42*, 15.
(44) Burrill, K. A.; Woods, D. R. *J. Colloid Interface Sci.* **1973**, *42*, 35.
(45) Chesters, A. K.; Hofman, G. *Appl. Sci. Res.* **1982**, *38*, 353. Chesters, A. K. *Chem. Eng. Res. Des.* **1991**, *69*, 259. Abid, S.; Chesters, A. K. *Int. J. Multiphase Flow* **1994**, *20*, 613.
(46) Lin, C. Y.; Slattery, J. C. *AIChE J.* **1982**, *28*, 786.
(47) Chen, J.; Hahn, P. S.; Slattery, J. C. *AIChE J.* **1984**, *30*, 622.
(48) Allan, R. S.; Mason, S. G. *Trans. Faraday Soc.* **1961**, *57*, 2027.
(49) Allan, R. S.; Mason, S. G. *J. Colloid Sci.* **1962**, *17*, 383.
(50) Janssen, J. M. H. Ph.D. Thesis, Eindhoven University of Technology, Eindhoven, The Netherlands, 1993.
(51) Ziff, Z. M. *Macromolecules* **1986**, *19*, 2513.
(52) Ramkrishna, D. *Rev. Chem. Eng.* **1985**, *3*, 49.
(53) Muralidhar, R.; Ramkrishna, D. *6th Eur. Conf. Mixing* **1988**, 213.
(54) Thomas, S.; Prud'homme, R. E. *Polymer* **1992**, *33*, 4260.
(55) Park, D. W.; Roe, R. J. *Macromolecules* **1991**, *24*, 5324.
(56) Yoshida, M.; Ma, J. J.; Min, K.; White, J. L.; Quirk, R. P. *Polym. Eng. Sci.* **1990**, *30*, 30.
(57) Endo, S.; Min, K.; White, J. L.; Kyu, T. *Polym. Eng. Sci.* **1986**, *26*, 45.
(58) Fayt, R.; Jérôme, R.; Teyssié, P. *Makromol. Chem.* **1986**, *187*, 837.
(59) Favis, B. D.; Chalifoux, J. P. *Polymer* **1988**, *29*, 1761.
(60) Nakayama, A.; Guegan, P.; Hirao, A.; Inoue, T.; Macosko, C. W. *Polym. Prepr. (Am. Chem. Soc., Div. Polym. Chem.)* **1993**, *34* (2), 840. Guegan, P.; Macosko, C. W.; Ishizone, T.; Hirao, A.; Nakahama, S. *Macromolecules* **1994**, *27*, 4993.
(61) Datta, S.; Lohse, D. J. *Macromolecules* **1993**, *26*, 2064.
(62) Mirabella, F. M., Jr. *J. Polym. Sci., Polym. Phys.* **1994**, *32*, 1205. Mirabella, F. M., Jr.; Barley, J. S. *J. Polym. Sci., Polym. Phys.* **1994**, *32*, 2187.
(63) Leibler, L. *Makromol. Chem., Macromol. Symp.* **1988**, *16*, 1.
(64) Vilgis, T. A.; Noolandi, J. *Macromolecules* **1990**, *23*, 2941.
(65) Noolandi, J. *Makromol. Chem., Rapid Commun.* **1991**, *12*, 517.
(66) Wang, Z. G.; Safran, S. A. *J. Phys. Fr.* **1990**, *51*, 185.
(67) Dan, N.; Tirrell, M. *Macromolecules* **1993**, *26*, 637.
(68) Anastasiadis, S. J.; Gancarz, I.; Koberstein, J. T. *Macromolecules* **1989**, *22*, 1449.
(69) Elemans, P. H. M.; Janssen, J. H. M.; Meijer, H. E. H. *J. Rheol.* **1990**, *34*, 1311.
(70) Wagner, M.; Wolf, B. A. *Polymer* **1993**, *34*, 1460.
(71) Sundararaj, U. Ph.D. Thesis, University of Minnesota, Minneapolis, MN, 1994.
(72) Chen, C. C.; White, J. L. *Polym. Eng. Sci.* **1993**, *33*, 923.
(73) Fleischer, C. A.; Morales, A. R.; Koberstein, J. T. *Macromolecules* **1994**, *27*, 379.
(74) Heikens, D.; Bartensen, W. *Polymer* **1977**, *18*, 69.
(75) Willis, J. M.; Favis, B. D.; Lunt, J. *Polym. Eng. Sci.* **1990**, *30*, 1073.
(76) Angola, J. C.; Fujita, Y.; Sakai, T.; Inoue, T. *J. Polym. Sci., Polym. Phys.* **1988**, *26*, 807.
(77) Padwa, A. R.; Wolske, K. W.; Sasaki, Y.; Macosko, C. W. *J. Polym. Sci., Polym. Chem.*, accepted for publication. Padwa, A. R.; Lavengood, R. E. *Polym. Prepr. (Am. Chem. Soc., Div. Polym. Chem.)* **1992**, *33* (2), 600.
(78) Sundararaj, U.; Macosko, C. W.; Shih, C. K. *Soc. Plast. Tech. Papers* **1992**, *50*, 1802.
(79) Liu, N. C.; Baker, W. E. *Adv. Polym. Technol.* **1992**, *11*, 249.
(80) Cruz-Orive, L. M. *J. Microsc.* **1976**, *107*, 235.
(81) Russ, J. C. *Practical Stereology*; Plenum Press: New York, 1986; Chapter 4.
(82) de Bruijn, R. A. Ph.D. Thesis, Eindhoven University of Technology, Eindhoven, The Netherlands, 1989.
(83) van Oene, H. *J. Colloid Interface Sci.* **1972**, *40*, 448.
(84) Milliken, W. J.; Leal, L. G. *J. Non-Newtonian Fluid Mech.* **1991**, *40*, 355.
(85) Tadros, T. F.; Vincent B. In *Encyclopedia of Emulsion Technology*; Becher, P., Ed.; Marcel Dekker Inc.: New York, 1988; Vol. 1, Chapter 3.
(86) Molau, G. E. *J. Polym. Sci., Part A* **1965**, *3*, 4235.
(87) Huneault, M. A.; Utracki, L. A. *Polym. Eng. Sci.* **1995**, in press.
(88) Scott, C. E.; Macosko, C. W. *Polymer* **1994**, *35*, 5422.

MA941323G